

Lawrence Berkeley National Laboratory

LBL Publications

Title

High pressure polymorphs and amorphization of upconversion host material NaY(WO₄)₂

Permalink

<https://escholarship.org/uc/item/7b9657rd>

Journal

Applied Physics Letters, 109(4)

ISSN

0003-6951

Authors

Hong, Fang
Yue, Binbin
Cheng, Zhenxiang
[et al.](#)

Publication Date

2016-07-25

DOI

10.1063/1.4960104

Peer reviewed



High pressure polymorphs and amorphization of upconversion host material NaY(WO₄)₂

Fang Hong, Binbin Yue, Zhenxiang Cheng, Martin Kunz, Bin Chen, and Ho-Kwang Mao

Citation: [Applied Physics Letters](#) **109**, 041907 (2016); doi: 10.1063/1.4960104

View online: <http://dx.doi.org/10.1063/1.4960104>

View Table of Contents: <http://scitation.aip.org/content/aip/journal/apl/109/4?ver=pdfcov>

Published by the [AIP Publishing](#)

Articles you may be interested in

[High pressure structural, electronic, and optical properties of polymorphic InVO₄ phases](#)

J. Appl. Phys. **119**, 085702 (2016); 10.1063/1.4942182

[High pressure synthesis of amorphous TiO₂ nanotubes](#)

AIP Advances **5**, 097128 (2015); 10.1063/1.4930916

[Exploring the high-pressure behavior of the three known polymorphs of BiPO₄: Discovery of a new polymorph](#)

J. Appl. Phys. **117**, 105902 (2015); 10.1063/1.4914407

[Amorphous polymorphs](#)

AIP Conf. Proc. **1447**, 51 (2012); 10.1063/1.4709880

[High-pressure phases of NaAlH₄ from first principles](#)

Appl. Phys. Lett. **100**, 061905 (2012); 10.1063/1.3682317

The image shows the cover of an Applied Physics Reviews journal. It features a 3D molecular model of a crystal structure in shades of blue and orange. The text 'AIP Applied Physics Reviews' is at the top left. The main title 'NEW Special Topic Sections' is in large white font. Below it, 'NOW ONLINE' is in yellow, followed by 'Lithium Niobate Properties and Applications: Reviews of Emerging Trends' in white. The AIP Applied Physics Reviews logo is at the bottom right.

NEW Special Topic Sections

NOW ONLINE
Lithium Niobate Properties and Applications:
Reviews of Emerging Trends

AIP Applied Physics Reviews

High pressure polymorphs and amorphization of upconversion host material $\text{NaY}(\text{WO}_4)_2$

Fang Hong,^{1,2} Binbin Yue,^{1,2,a)} Zhenxiang Cheng,³ Martin Kunz,² Bin Chen,^{1,a)} and Ho-Kwang Mao^{1,4}

¹Center for High Pressure Science and Technology Advanced Research, 1690 Cailun Rd. Pudong, Shanghai 201203, People's Republic of China

²The Advanced Light Source, Lawrence Berkeley National Laboratory, 1 Cyclotron Rd, Berkeley, California 94720, USA

³Institute for Superconducting and Electronic Materials, Australian Institute of Innovative Materials, University of Wollongong, Innovation Campus, Squires Way, North Wollongong, NSW 2500, Australia

⁴Geophysical Laboratory, Carnegie Institution of Washington, Washington, DC 20015, USA

(Received 30 June 2016; accepted 19 July 2016; published online 29 July 2016)

The pressure effect on the structural change of upconversion host material $\text{NaY}(\text{WO}_4)_2$ was studied by using *in-situ* synchrotron X-ray diffraction. A transition from the initial scheelite phase to the M-fergusonite phase occurs near 10 GPa, and another phase transition is found near 27.5 GPa, which could be an isostructural transition without symmetry change. The sample becomes amorphous when the pressure is fully released from high pressure. This work demonstrates the possibility of synthesizing various polymorph structures for non-linear optical applications with a high pressure, chemical doping, or strained thin-film nanostructure process. *Published by AIP Publishing.*
[\[http://dx.doi.org/10.1063/1.4960104\]](http://dx.doi.org/10.1063/1.4960104)

Photon upconversion is a nonlinear optical process where two or more low-energy photons have been sequentially absorbed by a material, and consequently, a high-energy light emission occurs.¹ The crystal structure of the parent materials hosting the light emission centers is very important for their optical performance.^{2–5} Nanostructured NaYF_4 has been used as a host for rare-earth-ion-luminescence upconversion, and these rare-earth-ion-doped NaYF_4 nanocrystals have promising applications in the fields of bio-imaging, sensing, cancer therapy, energy transfer, and even 3D display.^{6–11} The hexagonally structured NaYF_4 has better upconversion efficiency than the cubic structure due to its higher light absorption efficiency.⁷ The ABO_4 -type oxide materials are expected to have more advantages for high-power laser materials due to their stable thermal conductivity,¹² mechanical properties, light transparency, and easy access to large crystals.^{13–15} Lanthanide-doped CaWO_4 has been studied widely for its bright light emission.^{5,16,17} However, the chemical valences of most lanthanide ions are 3+, and these lanthanide ions locate inside the material interstitially, which limits the doping level and light emission effect. To enhance the upconversion performance, it is a good strategy to replace the Ca^{2+} by both Na^+ and RE^{3+} (RE = rare-earth elements). Based on this idea, $\text{NaY}(\text{WO}_4)_2$ (or $\text{Na}_{0.5}\text{Y}_{0.5}\text{WO}_4$) and $\text{NaGd}(\text{WO}_4)_2$ have been used as the host materials for solid-state laser materials.^{13–15,18–20} Unlike the structural instability of NaYF_4 induced by lanthanide-doping, the crystal structures of $\text{NaY}(\text{WO}_4)_2$ and $\text{NaGd}(\text{WO}_4)_2$ are both very stable because the doped lanthanide ions have a similar ionic radius and therefore their substitution does not affect the crystal structure. This allows the $\text{NaY}(\text{WO}_4)_2$ and $\text{NaGd}(\text{WO}_4)_2$ to be excellent host materials. In addition, AWO_4 -type materials can be used as detector

materials for α -ray and γ -rays and even for searching for dark matter or neutrinoless double beta decay.^{21,22}

To tune the emission bands and/or achieve a much higher upconversion effect potential in these kinds of materials, it is important to find a method to control the crystal structure of the host materials. Here, we employed high pressure to study the structural evolution of $\text{NaY}(\text{WO}_4)_2$ and found that there are two phase transitions near 10 GPa and 27.5 GPa, respectively. This work reveals possible high pressure polymorphic structures suitable for upconversion application and rare-event searches by using direct high pressure synthesis, chemical pressure introducing by smaller ion doping and strained structure-like epitaxial thin films.

A high-quality $\text{NaY}(\text{WO}_4)_2$ sample was synthesized by a solid state reaction method and ground into fine powder for this high pressure experiment. A compact sample was loaded in a Mao-type symmetric diamond anvil cell with a diamond culet of 300 μm . Silicone oil was used as a pressure medium. There are reports that the hydro-staticity of silicone oil is as good as the 4:1 methanol:ethanol mixture at low pressures to ~ 20 GPa and behaves as well as argon above 30 GPa.^{23,24} A stainless steel gasket was used, and a 100 μm sample hole was drilled with a laser drilling system. The pressure was monitored by the R1-R2 line shift of Ruby. The *in situ* synchrotron micro X-ray diffraction experiment was carried out at room temperature on Beamline 12.2.2 at the Advanced Light Source at the Lawrence Berkeley National Laboratory and the incident X-ray wavelength was 0.4959 Å. Further details on the experiment are given Ref. 25.

The structural evolution of the $\text{NaY}(\text{WO}_4)_2$ sample under high pressure was examined by X-ray diffraction and the results are presented in Figure 1. The X-ray diffraction pattern during the compression process is shown in Figure 1(a) while Figure 1(b) displays the decompression process. It is clear that there is a structural phase transition near 10 GPa

^{a)}Electronic addresses: yuebb@hpstar.ac.cn and chenbin@hpstar.ac.cn

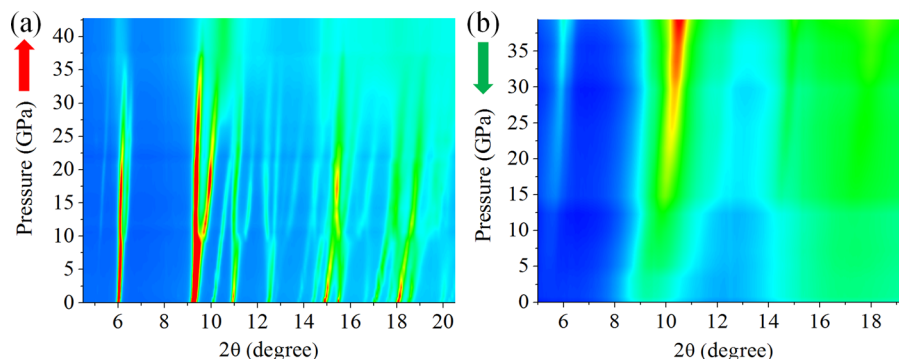


FIG. 1. The 2D x-ray diffraction mapping of $\text{NaY}(\text{WO}_4)_2$ at various pressures during compression and decompression, collected at room temperature. (a) The compression process: a clear structural phase transition is found near 10 GPa, evidenced by the appearance of extra peaks, and another phase transition starts near 27.5 GPa, indicated by an extra peak near $2\theta = 6^\circ$ and peak broadening; (b) decompression process: the peak intensity decreases as pressure releases and the sample becomes amorphous when the pressure is fully released.

during the compression process, where some extra peaks appear. In addition, an extra peak is found near $2\theta = 6^\circ$, and a shoulder peak appears near $2\theta = 10^\circ$ when the pressure reaches above 27.5 GPa. These changes suggest another phase transition. Under ambient conditions, the sample crystallizes in the scheelite-type tetragonal structure with a space group of $I4_1/a$, and the lattice parameters are $a = 5.20479 \text{ \AA}$ and $c = 11.27159 \text{ \AA}$ according to the Rietveld refinement. These values are very similar to those of CaWO_4 .²⁶ Upon compression, all diffraction peaks of the tetragonal structure shift to higher angles, indicating that both the a and c axes become shorter under pressure. Some peaks shift faster than others, which suggests that the compressibility of the a and c axes differs from each other. Near 10 GPa, another phase appears and can be assigned to a monoclinic structure with a space group of $I2/a$, which is a typical M-fergusonite-type phase. A similar transition sequence from the scheelite phase to the M-fergusonite phase has also been observed in CaWO_4 , SrWO_4 , and YLiF_4 .^{26,27} The diffraction peaks of the M-fergusonite-type phase shift to higher angles upon compression. At higher pressure (above 27.5 GPa), the peaks broaden and the intensity decreases as well. To some extent, the third phase is mixed with the M-fergusonite phase at a certain pressure range. As shown in Figure 1(b), during the decompression process, the third phase is maintained for a wide pressure range and does not go back to the M-fergusonite-type phase. However, the intensity continuously declines and the sample becomes amorphous when pressure is fully released.

Figure 2(a) displays the Rietveld refinement of x-ray diffraction patterns collected at three representative pressures. At 5.3 GPa, the structure is still in the tetragonal phase, marked as T, which is the stable phase in ambient conditions. The peak position is well matched, and there is a relatively big difference between the experimental data and calculated data due to the higher contribution of some large grains. At 15.8 GPa, the structure already transfers to the M-fergusonite-type monoclinic structure, marked as M1. Due to the crack of big grains, the intensity difference between the experimental data and calculation data becomes much smaller than at 5.3 GPa. At 33.6 GPa, the M-fergusonite-type is mixed with another monoclinic phase with the same space group. The third phase is marked as M2 in the figure.

We tried to assign the third phase as the orthorhombic structure with space group Cmca , proposed by Botella *et al.* for the high pressure phase found in CaWO_4 .²⁸ However, the parameters provided in their work do not give a good refinement, even if we completely free the main structure parameters, because some extra peaks will appear at low diffraction angle region between $2\theta = 7^\circ$ and $2\theta = 9^\circ$. In our experimental data, there is no extra peak in that region. The situation is almost same when we assigned this high pressure phase to the Wolframite-type phase.^{29,30} Considering this character, we assume that the symmetry may not change, but the lattice parameter and atomic position do change. Then, we can get a good refinement result with two monoclinic structures (with the same symmetry $I2/a$) with different unit cell parameters. Hence, we proposed that the second high pressure polymorph of $\text{NaY}(\text{WO}_4)_2$ is still in a monoclinic structure with space group $I2/a$. Here, we cannot exclude another structural possibility due to the weak intensity and broad peak of the second high pressure phase, and a further study is required to examine the accurate structure. All the atomic

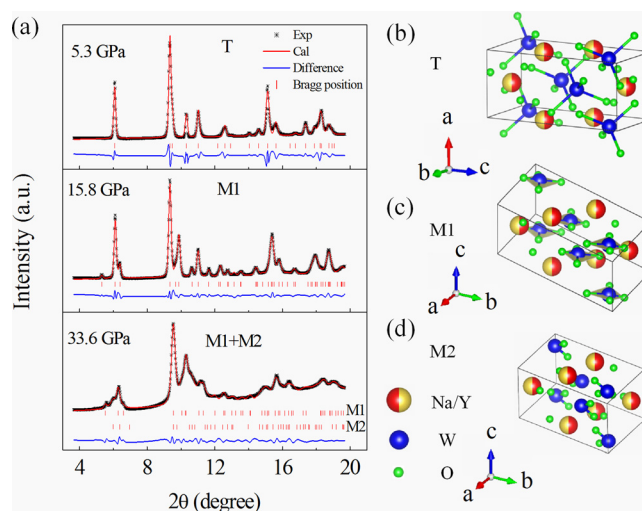


FIG. 2. The Rietveld refinement of the X-ray powder diffraction pattern at representative pressures and the atomic structure of three different phases. (a) At 5.3 GPa, the sample has a tetragonal structure, space group $I4_1/a$; at 15.8 GPa, it changes into a monoclinic structure with space group $I2/a$; at 33.6 GPa, an extra monoclinic phase appears with the same symmetry; (b–d) atomic structure of unit cell of tetragonal phase (T), monoclinic phase 1 (M1), and monoclinic phase 2 (M2), respectively.

TABLE I. Structural data of NaY(WO₄)₂ obtained from the Rietveld refinement of the x-ray powder diffraction pattern at representative pressures.

5.3 GPa					
T (<i>I</i> ₄₁ / <i>a</i>)		a	b	c	
		5.162 (8)	5.162 (8)	11.032 (7)	
15.8 GPa					
M1 (<i>I</i> ₂ / <i>a</i>)		a	b	c	Beta
		4.908 (1)	10.693 (4)	5.183 (7)	94.553 (9)
33.6 GPa					
M2 (<i>I</i> ₂ / <i>a</i>)		a	b	c	Beta
		5.929 (3)	8.161 (3)	5.417 (3)	79.391 (1)

	Site	x	y	z	Occupancy
Na	4b	0	0.25	0.625	0.5
Y	4b	0	0.25	0.625	0.5
W	4a	0	0.25	0.125	1
O	16f	0.2118 (6)	-0.1068 (1)	-0.0076 (4)	1

	Site	x	y	z	Occupancy
Na	4e	0.25	0.6556 (9)	0	0.5
Y	4e	0.25	0.6556 (9)	0	0.5
W	4e	0.25	0.1321 (1)	0	1
O1	8f	0.4395 (7)	0.0474 (4)	0.1030 (9)	1
O2	8f	0.5477(7)	0.2991 (0)	0.6878 (2)	1

	Site	x	y	z	Occupancy
Na	4e	0.25	0.5389 (6)	0	0.5
Y	4e	0.25	0.5389 (6)	0	0.5
W	4e	0.25	0.1135 (6)	0	1
O1	8f	-0.0839 (6)	0.1807 (5)	-0.4452 (9)	1
O2	8f	0.9619(5)	-0.2184(2)	0.5939(9)	1

structures of these three phases are demonstrated in Figures 2(b)–2(d), respectively. Meanwhile, the main structure parameters based on Rietveld refinement results are listed in Table I (shown at the end of this manuscript for review).

The detailed structural information at different pressures is provided in Figure 3. The pressure dependent lattice parameters are plotted in Figure 3(a). Consistent with the

discussion mentioned above, the lattice parameters of the T phase decrease monotonously upon high pressure but they show different compressibilities. The *cla* ratio decreases with pressure (not shown), suggesting that the longer *c* axis is more easily compressed than the short *a* axis. When the pressure exceeds 10 GPa, the M1 phase appears and the previous *c* axis in the T phase becomes a *c* axis in the M1 phase due to the symmetry change. All three lattice parameters in the M1 phase show a monotonously declining trend with pressure. The trend changes a little bit for the *b* axis when the sample enters into the M2 phase, which shows a positive dependence at first for a few pressure points and then decreases with pressure. The pressure dependent volume change is given in Figure 3(b) (red solid cubic: T phase; blue solid circle: M1 phase; magenta solid triangle: M2 phase; and olive green open circle: mixed M1 and M2 phase). The volumes become smaller and smaller with increasing pressure. Unlike a previous study on CaWO₄, we found a volume discontinuity near 10 GPa, where the T-M1 phase transition occurs.²⁶ For the M1-M2 phase transition, no volume discontinuity is observed. The pure M2 phase's volume is a little bit bigger than the pure M1 phase at the same pressure. It is noticed that the real volume (per unit) of the sample contributed by both M1 and M2 phases does not change too much above the M1-M2 phase transition pressure. This could be a signature of an amorphous process in the high pressure range. Pressure-driven volume anomaly has been observed in amorphous selenium and the local topological fluctuations during phase transition are proposed to be the origin of the anomaly.³¹ There is also a similar pressure-driven volume anomaly in amorphous silica and the network flexibility hypothesis could explain this anomaly.³² We speculate that the network flexibility at high pressure is responsible for the observed volume anomaly and finally allows the occurrence of amorphization. The disruption of some W-O bonds in M2 phase, as shown in Figure 2(d), already shows some signatures of amorphization. This is very similar to the case of

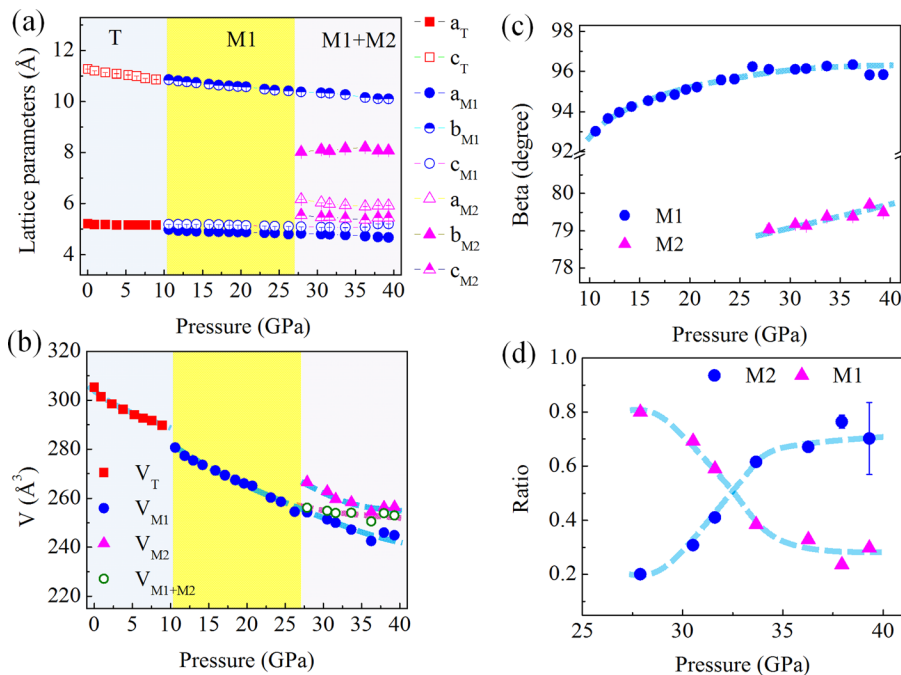


FIG. 3. The pressure dependent structural parameters obtained from the Rietveld refinement of the X-ray powder diffraction patterns. (a) The lattice parameter change under high pressure, (b) volume change, (c) the beta angle evolution of monoclinic structure from 10 GPa to 40 GPa, and (d) ratio of M1 and M2 phases above 27.5 GPa.

pressure-induced amorphous Ta₂O₅, in which the disruption of some weak-bonds initiates the amorphization.³³ Further work is required to determine an accurate crystal structure and clarify the volume anomaly. Figure 3(c) shows the beta angle of two monoclinic phases. The beta angle of the M1 phase is larger than 90°, and the beta angle of the M2 phase is smaller than 90°, but both of them show positive pressure dependence. The beta angle trend of the M1 phase is highly similar to the calculated result on the high pressure structure of CaWO₄.²⁸ The ratio of these two monoclinic phases is displayed in Figure 3(d). The ratio of the M2 phase increases sharply below 35 GPa and there is still a small portion of the M1 phase near 40 GPa, above which it is supposed to be a pure M2 phase and then the sample could enter into an amorphous state.

The M-fergusonite-type monoclinic (M1 phase) tungstates are found to exist in ambient conditions, such as HgWO₄ and KY(WO₄)₂.^{34–38} In lanthanide-doped monoclinic KY(WO₄)₂, highly efficient pulse laser operation has been achieved with a diode-pump.^{37,39} This precludes the possibility to continuously tune the crystal structure of NaY(WO₄)₂ by chemical doping via the introduction of different amounts of K or Hg at ambient conditions, which could boost the exploration of host materials for highly efficient upconversion and solid state lasers. In our study, even without K or Hg doping, the structure of NaY(WO₄)₂ can still be tuned continuously by external pressure, which provides another efficient way to do the same work. Amorphous materials have also been used as the host materials for upconversion and solid state lasers, such as amorphous silicon, Al₂O₃, and Y₂O₃.^{40–43} It is known that local crystal field affects the upconversion efficiency and it is very important to understand its effect on the luminescent properties. One solution is to synthesize both the bulk and amorphous host materials and make a comparative study. In some cases, the amorphous host materials perform better than the crystalline bulk materials, which make amorphous host materials more promising in some areas.^{40,44} Taking Y₂O₃, for example, the pulsed laser induces an amorphous surface layer on the Y₂O₃ nanocrystals and a strong blue light emission is observed when it is pumped by a 976 nm diode laser, which is ten times stronger than that of pure crystalline Y₂O₃.⁴⁰ Here, the amorphous NaY(WO₄)₂ was obtained by compression and the structure maintained at ambient conditions, suggesting that it could be a promising amorphous host material. Future luminescent studies based on this amorphous material could help us to understand the crystal field effect and provide more information on how to design high-performance optical materials for nonlinear optics.

The crystal structure of upconversion host material NaY(WO₄)₂ under high pressure has been studied via synchrotron x-ray diffraction at room temperature. At ambient conditions, NaY(WO₄)₂ is in the form of scheelite-type tetragonal structure. There is a structural phase transition, starting near 10 GPa, from the scheelite phase to the M-fergusonite phase. The M-fergusonite-type monoclinic structure is stable up to 27.5 GPa, above which the sample undergoes another structural phase transition. The second phase transition is proposed to be an isostructure transition without symmetry change, but the unit cells are quite different. The sample

becomes amorphous when pressure returns to ambient conditions, which could be explained by the volume anomaly of high pressure monoclinic structures. This work provides guidance on tuning the crystal structure of host materials for photon upconversion by using high pressure technique. This may inspire the chemical or physical synthesis of high pressure polymorphs by using direct high pressure synthesis, chemical doping, and strain engineering, and brighten the future applications of these kinds of host materials.

The authors acknowledge support from the NSAF (Grant No. U1530402). F.H. and B.B.Y. acknowledge the usage of beam time at Beamline 12.2.2 at the Advanced Light Source in Lawrence Berkeley National Laboratory. All authors thank Freyja O'Toole for her careful revision of the manuscript.

- ¹F. Auzel, *Chem. Rev.* **104**, 139–173 (2004).
- ²M. Haase and H. Schaefer, *Angew. Chem., Int. Ed.* **50**, 5808–5829 (2011).
- ³F. Wang, R. Deng, J. Wang, Q. Wang, Y. Han, H. Zhu, X. Chen, and X. Liu, *Nat. Mater.* **10**, 968–973 (2011).
- ⁴H. Wang, C. Tu, Z. You, F. Yang, Y. Wei, Y. Wang, J. Li, Z. Zhu, G. Jia, and X. Lu, *Appl. Phys. B* **88**, 57–60 (2007).
- ⁵J. H. Chung, S. Y. Lee, K. B. Shim, and J. H. Ryu, *Appl. Phys. Express* **5**, 052602 (2012).
- ⁶B. Zhou, B. Shi, D. Jin, and X. Liu, *Nat. Nanotechnol.* **10**, 924–936 (2015).
- ⁷F. Wang, Y. Han, C. S. Lim, Y. Lu, J. Wang, J. Xu, H. Chen, C. Zhang, M. Hong, and X. Liu, *Nature* **463**, 1061–1065 (2010).
- ⁸F. Wang and X. Liu, *Chem. Soc. Rev.* **38**, 976–989 (2009).
- ⁹J. Zhou, Z. Liu, and F. Li, *Chem. Soc. Rev.* **41**, 1323–1349 (2012).
- ¹⁰F. Wang and X. Liu, *J. Am. Chem. Soc.* **130**, 5642 (2008).
- ¹¹W. Zou, C. Visser, J. A. Maduro, M. S. Pshenichnikov, and J. C. Hummelen, *Nat. Photonics* **6**, 560–564 (2012).
- ¹²A. Senyshyn, H. Kraus, V. B. Mikhailik, and V. Yakovyna, *Phys. Rev. B* **70**, 214306 (2004).
- ¹³F. Song, L. Han, H. Tan, J. Su, J. Yang, J.-g. Tian, G.-y. Zhang, Z.-x. Cheng, and H.-c. Chen, *Opt. Commun.* **259**, 179–186 (2006).
- ¹⁴M. D. Serrano, C. Cascales, X. Han, C. Zaldo, A. Jezowski, P. Stachowiak, N. Ter-Gabrielyan, V. Fromzel, and M. Dubinskii, *PLoS One* **8**, e59381 (2013).
- ¹⁵J. Liu, H. Zhang, J. Wang, and V. Petrov, *Opt. Express* **15**, 12900–12904 (2007).
- ¹⁶W. Xu, X. Gao, L. Zheng, P. Wang, Z. Zhang, and W. Cao, *Appl. Phys. Express* **5**, 072201 (2012).
- ¹⁷W. Xu, Z. Zhang, and W. Cao, *Opt. Lett.* **37**, 4865–4867 (2012).
- ¹⁸X. Yu, Y. Qin, M. Gao, L. Duan, Z. Jiang, L. Gou, P. Zhao, and Z. Li, *J. Lumin.* **153**, 1–4 (2014).
- ¹⁹Z. Wang, Y. Li, Q. Jiang, H. Zeng, Z. Ci, and L. Sun, *J. Mater. Chem. C* **2**, 4495–4501 (2014).
- ²⁰Y. Wang, W. Xu, S. Cui, S. Xu, Z. Yin, H. Song, P. Zhou, X. Liu, L. Xu, and H. Cui, *Nanoscale* **7**, 1363–1373 (2015).
- ²¹Y. G. Zdesenko, F. T. Avignone Iii, V. B. Brudanin, F. A. Danevich, V. V. Kobychov, B. N. Kropivnyansky, S. S. Nagornyy, V. I. Tretyak, and T. Vyllov, *Astropart. Phys.* **23**, 249–263 (2005).
- ²²M. v. Sivers, M. Clark, P. C. F. Di Stefano, A. Erb, A. Gütlein, J.-C. Lanfranchi, A. Münster, P. Nadeau, M. Piquemal, W. Potzel, S. Roth, K. Schreiner, R. Strauss, S. Wawoczny, M. Willers, and A. Zöller, *J. Appl. Phys.* **118**, 164505 (2015).
- ²³Y. Shen, R. S. Kumar, M. Pravica, and M. F. Nicol, *Rev. Sci. Instrum.* **75**, 4450–4454 (2004).
- ²⁴S. Klotz, J. C. Chervin, P. Munsch, and G. L. Marchand, *J. Phys. D: Appl. Phys.* **42**, 075413 (2009).
- ²⁵M. Kunz, A. A. MacDowell, W. A. Caldwell, D. Cambie, R. S. Celestre, E. E. Doming, R. M. Duarte, A. E. Gleason, J. M. Glossinger, N. Kelez, D. W. Plate, T. Yu, J. M. Zaug, H. A. Padmore, R. Jeanloz, A. P. Alivisatos, and S. M. Clark, *J. Synchrotron Radiat.* **12**, 650–658 (2005).
- ²⁶D. Errandonea, J. Pellicer-Porres, F. J. Manjón, A. Segura, C. Ferrer-Roca, R. S. Kumar, O. Tschauner, P. Rodríguez-Hernández, J. López-Solano, S. Radescu, A. Mujica, A. Muñoz, and G. Aquilanti, *Phys. Rev. B* **72**, 174106 (2005).

- ²⁷A. Grzechnik, K. Syassen, I. Loa, M. Hanfland, and J. Y. Gesland, *Phys. Rev. B* **65**, 104102 (2002).
- ²⁸P. Botella, R. Lacomba-Perales, D. Errandonea, A. Polian, P. Rodríguez-Hernández, and A. Muñoz, *Inorg. Chem.* **53**, 9729–9738 (2014).
- ²⁹R. Lacomba-Perales, D. Errandonea, D. Martínez-García, P. Rodríguez-Hernández, S. Radescu, A. Mujica, A. Muñoz, J. C. Chervin, and A. Polian, *Phys. Rev. B* **79**, 094105 (2009).
- ³⁰J. Ruiz-Fuertes, S. Lopez-Moreno, D. Errandonea, J. Pellicer-Porres, R. Lacomba-Perales, A. Segura, P. Rodríguez-Hernández, A. Muñoz, A. H. Romero, and J. Gonzalez, *J. Appl. Phys.* **107**, 083506 (2010).
- ³¹H. Liu, L. Wang, X. Xiao, F. De Carlo, J. Feng, H.-k. Mao, and R. J. Hemley, *Proc. Natl. Acad. Sci. U.S.A.* **105**, 13229–13234 (2008).
- ³²M. W. Andrew, A. S. Lucy, T. Kostya, P. B. Richard, O. H. W. Toby, T. D. Martin, P. T. Richard, T. T. Ilian, and A. W. Stephen, *J. Phys.: Condens. Matter* **19**, 275210 (2007).
- ³³X. Lü, Q. Hu, W. Yang, L. Bai, H. Sheng, L. Wang, F. Huang, J. Wen, D. J. Miller, and Y. Zhao, *J. Am. Chem. Soc.* **135**, 13947–13953 (2013).
- ³⁴F. J. Manjón, J. López-Solano, S. Ray, O. Gomis, D. Santamaría-Pérez, M. Mollar, V. Panchal, D. Errandonea, P. Rodríguez-Hernández, and A. Muñoz, *Phys. Rev. B* **82**, 035212 (2010).
- ³⁵K. K. Rasu, A. Durairajan, D. Balaji, and S. M. Babu, *AIP Conf. Proc.* **1665**, 140007 (2015).
- ³⁶P. A. Loiko, V. I. Dashkevich, S. N. Bagaev, V. A. Orlovich, A. S. Yasukevich, K. V. Yumashev, N. V. Kuleshov, E. B. Dunina, A. A. Kornienko, S. M. Vatnik, and A. A. Pavlyuk, *J. Lumin.* **153**, 221–226 (2014).
- ³⁷E. Castellano-Hernandez, X. Han, M. Rico, L. Roso, C. Cascales, and C. Zaldo, *Opt. Express* **23**, 11135–11140 (2015).
- ³⁸R. Cattoor, I. Manek-Hoenninger, D. Rytz, L. Canioni, and M. Eichhorn, *Opt. Lett.* **39**, 6407–6410 (2014).
- ³⁹T. C. Schratwieser, C. G. Leburn, and D. T. Reid, *Opt. Lett.* **37**, 1133–1135 (2012).
- ⁴⁰C. B. Zheng, Y. Q. Xia, F. Qin, Y. Yua, J. P. Miao, Z. G. Zhang, and W. W. Cao, *Chem. Phys. Lett.* **509**, 29–32 (2011).
- ⁴¹Y. Y. Cheng, B. Fueckel, R. W. MacQueen, T. Khoury, R. G. C. R. Clady, T. F. Schulze, N. J. Ekins-Daukes, M. J. Crossley, B. Stannowski, K. Lips, and T. W. Schmidt, *Energy Environ. Sci.* **5**, 6953–6959 (2012).
- ⁴²L. Agazzi, K. Worhoff, and M. Pollnau, *J. Phys. Chem. C* **117**, 6759–6776 (2013).
- ⁴³J. de Wild, A. Meijerink, J. K. Rath, W. G. J. H. M. van Sark, and R. E. I. Schropp, *Sol. Energy Mater.* **94**, 1919–1922 (2010).
- ⁴⁴G. S. Qin, W. P. Qin, C. F. Wu, S. H. Huang, J. S. Zhang, S. Z. Lu, D. Zhao, and H. Q. Liu, *J. Appl. Phys.* **93**, 4328–4330 (2003).